Structure of Nonionic Surfactant Micelles in the Ionic Liquid Ethylammonium Nitrate

Miguel U. Araos and Gregory G. Warr*

School of Chemistry, The University of Sydney, Sydney, NSW, 2006, Australia

Received May 25, 2008. Revised Manuscript Received June 17, 2008

The structure of micelles formed by nonionic polyoxyethylene alkyl ether nonionic surfactants, C_nE_m, in the room-temperature ionic liquid, ethylammonium nitrate (EAN), has been determined by small-angle neutron scattering (SANS) as a function of alkyl and ethoxy chain length, concentration, and temperature. Micelles are found to form for all alkyl chains from dodecyl through to octadecyl. Dodecyl-chained surfactants have high critical micelle concentrations, around 1 wt%, and form weakly structured micelles. Surfactants with longer alkyl chains readily form micelles in EAN. The observed micelle structure changes systematically with alkyl and ethoxy chain length, in parallel with observations in aqueous solutions. Decreasing ethoxy chain length at constant alkyl chain length leads to a sphere to rod transition. These micelles also grow into rods with increasing temperature as their cloud point is approached in EAN.

Introduction

Over the past several years there has been an upsurge in interest in room temperature ionic liquids, or molten salts, as solvents for organic and inorganic synthesis, largely focused on imidazolium derivatives. This has mainly been based around their "green" pedigree, due to their negligible vapor pressure, and to their tunability as solvents by ready incorporation of one or more functional groups.[1–3] There are a few recent studies of surfactant behavior in such ionic liquids, but the amount of attention paid to this is miniscule compared with the burgeoning literature on synthesis. Although there is mounting evidence in favor of self-assembly by small surfactant molecules in imidazolium and related ionic liquids,[4,5] micelles have not been unambiguously shown to exist. However, there is good evidence for vesicle formation in an ether-containing imidazolium ionic liquid, making a strong case for purely "ionophobic" surfactant self-assembly.[6] In contrast with this, the formation of block copolymer micelles of poly(butadiene-*b*-ethylene oxide)[7] and liquid crystals of poly(ethylene oxide-*b*-propylene oxide-*b*-ethylene oxide)[8] in imidazolium ionic liquids is well established.

Ethylammonium nitrate (EAN) is a room-temperature ionic liquid whose behavior is in striking contrast to more widely studied ionic liquids. Self-assembly of surfactants into micelles,[9,10] and of lipids into lamellar liquid crystal phases,[11–13] in EAN was clearly demonstrated to occur over 20 years ago. Unlike most ionic liquids of current synthetic interest, EAN is protic and has the potential to form a three-dimensional hydrogen-bond network, which was postulated to be an essential feature in supporting surfactant self-assembly.[14] We have recently demonstrated the existence of lyotropic phases[15] and microemulsions[16] of nonionic surfactants and structured adsorbed layers at solid/liquid interfaces[17] in EAN.

In this paper we systematically explore micelle formation by nonionic surfactants in EAN using small angle neutron scattering. Using polyoxyethylene surfactants, C_nE_m, with a range of alkyl and ethoxy chain lengths so that molecular structure is systematically varied, we map out the kinds of micelles formed and relate this to their well-known behavior in aqueous systems.

Self-assembly structures, and particularly systematic trends in micelle morphology, can be rationalized using the surfactant packing parameter,[18] v/a_0l_c, where v is the volume of a surfactant hydrocarbon tail, a_0 is the effective area per headgroup, and l_c is the fully extended alkyl chain length. l_c forms an upper bound on the radius of a spherical or cylindrical micelle, or the half-thickness of a bilayer. Spherical micelles form for a packing parameter less than or equal to one-third, rod-like micelles form for a packing parameter between one-third and one-half, and bilayers form for a packing parameter between one-half and one. Thus, as ethoxylation number, and hence a_0, is increased at fixed alkyl chain (v and l_c), the micelle morphology is expected to change toward higher curvature: from planar to rod-like to spherical. Increasing alkyl chain length at fixed a_0 causes a slight decrease in aggregate curvature.

As the temperature is increased toward the cloud point in aqueous solution, nonionic surfactants exhibit micellar growth.[19–21] The exact nature of micelle behavior in this region has not been fully explained, but it is widely believed that as the

* Author for correspondence: g.warr@chem.usyd.edu.au.

(1) Forsyth, S. A.; Pringle, J. M.; MacFarlane, D. R. *Aust. J. Chem.* **2004**, *57*, 113.
(2) Rogers, R. D.; Seddon, K. R. *Science* **2003**, *302*, 792.
(3) Seddon, K. R.; Stark, A.; Torres, M.-J. *Pure Appl. Chem.* **2000**, *72*, 2275.
(4) Hao, J. ; Zemb, Th.N. *Curr. Opin. Colloid Interface Sci.* **2007**, *12*, 129–137.
(5) Fletcher, K. A.; Pandey, S. *Langmuir* **2004**, *20*, 33.
(6) Nakashima, T.; Kimizuka, N. *Chem. Lett.* **2002**, 1018.
(7) He, Y. Y.; Li, Z. B.; Simone, P.; Lodge, T. P. *J. Am. Chem. Soc.* **2006**, *128*, 2745.
(8) Wang, L.; Chen, X.; Chai, Y.; Hao, J.; Sui, Z.; Zhuang, W.; Sun, Z. *Chem. Commun.* **2004**, 2840.
(9) Evans, D. F.; Yamauchi, A.; Roman, R.; Casassa, E. Z. *J. Colloid Interface Sci.* **1982**, *88*, 89.
(10) Evans, D. F.; Yamauchi, A.; Wei, G. J.; Bloomfield, V. A. *J. Phys. Chem.* **1983**, *87*, 3537.
(11) Evans, D. F.; Kaler, E. W.; Benton, W. J. *J. Phys. Chem.* **1983**, *87*, 533.
(12) Tamura-Lis, W.; Lis, L. J.; Quinn, P. J. *J. Phys. Chem.* **1987**, *91*, 4625.
(13) Tamura-Lis, W.; Lis, L. J.; Quinn, P. J. *Biophys. J.* **1988**, *53*, 489.
(14) Evans, D. F.; Chen, S.-H.; Schriver, G. W.; Arnett, E. M. *J. Am. Chem. Soc.* **1981**, *103*, 481.
(15) Araos, M. U.; Warr, G. G. *J. Phys. Chem. B.* **2005**, *109*, 14275.
(16) Atkin, R.; Warr, G. G. *J. Phys. Chem. B* **2007**, *111*, 9309.
(17) Atkin, R.; Warr, G. G. *J. Am. Chem. Soc.* **2005**, *127*, 11940.
(18) Israelachvili, J. N.; Mitchell, J. D.; Ninham, B. W. *J. Chem. Soc., Faraday Trans. 2* **1976**, *72*, 1525.
(19) Magid, L. J.; Triolo, R.; Johnson, J. S., Jr *J. Phys. Chem.* **1984**, *88*, 5730.
(20) Lum Wan, J. A.; Warr, G. G.; White, L. R.; Grieser, F. *Colloid Polym. Sci.* **1988**, *265*, 528.
(21) Triolo, R.; Magid, L. J.; Johnson, J. S., Jr.; Child, H. R. *J. Phys. Chem.* **1982**, *86*, 3689.

10.1021/la801603t CCC: $40.75
Published on Web 08/05/2008

cloud temperature is approached the polyoxyethylene head groups begin to dehydrate,[22] which decreases a_0. This leads to a sphere-to-rod transition, and there is good evidence for a rod to branched-rod or network transition near the cloud temperature from electron microscopy[23,24] and atomic force microscopy.[25]

We have also chosen these nonionic surfactants particularly as they address this central issue of the role of H-bonding in solvophobic self-assembly. Their polyether hydrophilic moiety may be solvated by the H-bonding to the ethylammonium cation, giving them a stronger amphiphilic character in EAN than in non-H-bonding ionic liquids. These C_nE_m/EAN mixtures also exhibit a lower consolute boundary, and hence a cloud point,[15] which suggests that the temperature-dependence of micelle structure in EAN may also parallel aqueous systems.

Experimental Section

Polyoxyethylene alkyl ether nonionic surfactants, C_nE_m, of various alkyl chain lengths, n, and degrees of ethoxylation, m, were purchased from Nikkol or Fluka and were used as received. Purity was verified by reverse-phase HPLC. Samples were stored n a vacuum desiccator and their dryness verified from time to time by Karl Fischer titration.

d_5-Ethylammonium nitrate ($C_2D_5NH_3NO_3$, d_5-EAN) was prepared as described previously for hydrogenous EAN[9] by slow addition of concd nitric acid to d_5-ethylamine (CDN isotopes) solution chilled in ice. The product was rotary evaporated, freeze-dried to remove water, and then stored under nitrogen. The water content, determined by Karl Fischer titration, was around 0.7% v/v.

Small angle neutron scattering (SANS) was performed on the NG3 beamline at the Center for Neutron Research at NIST, Gaithersburg, MD.[26] Neutrons with an average wavelength of 6.0 Å and a $\Delta\lambda/\lambda = 15\%$ were selected with a velocity selector. Scattering was from 1.0 mm path-length samples onto a 650 × 650 mm^2 2D detector with 128 × 128 elements. The detector was offset by 0.2 m and scattering collected at two distances (1.4 and 13.1 m), giving a combined Q range of 0.0038 to 0.371 Å^{-1}. Raw SANS data was corrected for empty cell scattering, radially averaged and scaled to absolute intensity using standard procedures. Scattered intensity from d_5-EAN was independent of Q over the entire detector, except very close to the beamstop. The total background was calculated from the gradient of IQ^4 versus Q^4,[27,28] and has been subtracted from all spectra shown. All data were fitted using the Igor routines provided by NIST, as discussed further below.[29]

Results

$C_{12}E_m$ Surfactants. Small-angle neutron scattering spectra of 1 wt% solutions of $C_{12}E_m$ with $m = 5, 6, 8$ are shown in Figure 1. Several spectra were recorded over the temperature range 25−70 °C, but only three representative curves are shown.

SANS spectra of micellar solutions are usually interpreted by separating the scattering into a form factor, $P(Q)$, describing scattering by individual micelles, and a structure factor, $S(Q)$, due to correlations between micelles arising from intermicellar interactions.[30]

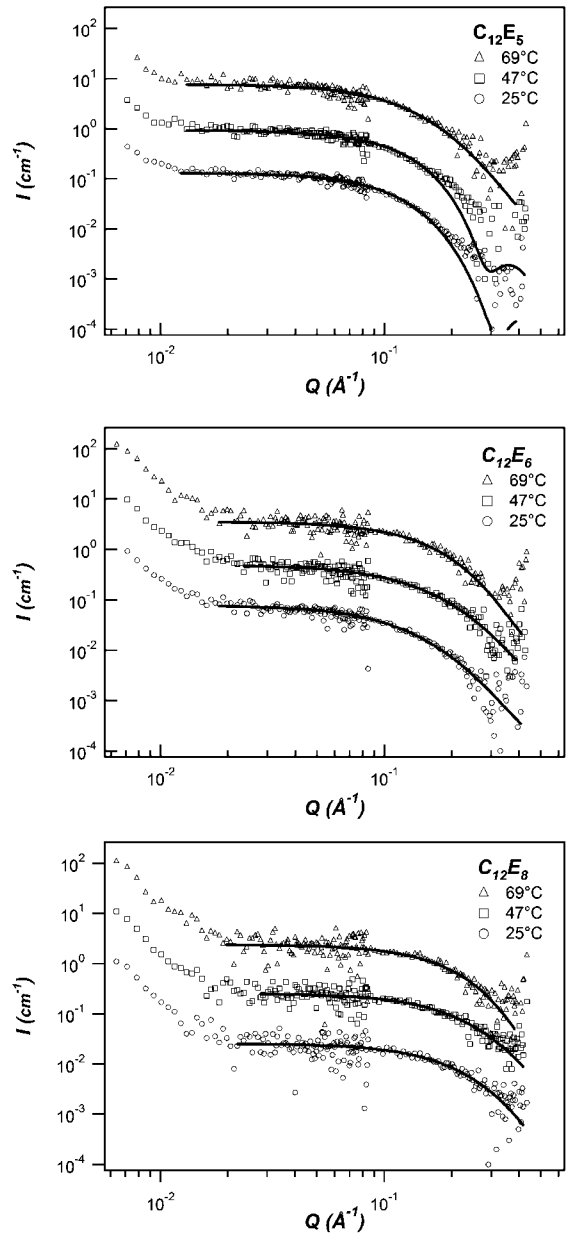

Figure 1. Small angle neutron scattering spectra of 1 wt% solutions of (a) $C_{12}E_5$, (b) $C_{12}E_6$, and (c) $C_{12}E_8$ in $C_2D_5NH_3NO_3$ (d_5-EAN) at 25, 47, and 69 °C. Solid lines show fits to a polydisperse core−shell spheres model with the parameters listed in Table 1 For clarity, data at 47 and 69 °C were scaled by factors of 10 and 100, respectively.

$$I(Q) = N_P(V_{mic}\Delta\rho)^2 P(Q)S(Q)$$

where N_P is the number density of micelles, $\Delta\rho$ is the scattering contrast between the micelle core and solvent, and $Q = (4\pi/\lambda)\sin\theta$, where 2θ is the scattering angle and λ is the neutron wavelength. SANS spectra of 1 wt% dodecyl surfactant solutions, shown in Figure 1, were fitted to a model of polydisperse a (Schulz) distribution of spheres of fixed core:shell ratio,[30] neglecting the effect of micelle−micelle correlations at these very high dilutions. These spectra also show an upturn at low Q not present in pure d_5-EAN. We attribute this to small bubbles of the surface of the cells stabilized by surfactant and only visible in dilute solutions of highly soluble ($C_{12}E_m$) surfactants with extremely low (<0.1 cm^{-1}) coherent scattered intensity. We have found EAN to be autophobic on silica surfaces, facilitating bubble adhesion.

Typical micelle sizes are near the resolution limit of these experiments; hence, we have constrained our models for all

(22) Mitchell, J. D.; Tiddy, G. J. T.; Waring, L.; Bostock, T.; McDonald, M. P. *Faraday Trans. 1* **1983**, *79*, 975.
(23) Bernheim-Groswasser, A.; Tlusty, T.; Safran, S. A.; Talmon, Y. *Langmuir* **1999**, *15*, 5448.
(24) Tlusty, T.; Safran, S. A.; Menes, R.; Strey, R. *Phys. Rev. Lett.* **1997**, *78*, 2616.
(25) Blom, A.; Warr, G. G.; Wanless, E. J. *Langmuir* **2005**, *21*, 11850.
(26) Glinka, C. J.; Barker, J. G.; Hammouda, B.; Krueger, S.; Moyer, J. J.; Orts, W. J. *J. Appl. Crystallogr.* **1998**, *31*, 430.
(27) Porod, G. *Kolloid-Z.* **1951**, *124*, 83.
(28) Porod, G. *Kolloid-Z.* **1952**, *125*, 51.
(29) Kline, S. R. *J. Appl. Crystallogr.* **2006**, *39*, 895.
(30) Hayter, J. B. In *Physics of Amphiphiles: Micelles, Vesicles, and Microemulsions*; Degiorgio, V., Corti, M.,. Eds., Elsevier Science: New York, 1983.

Table 1. Derived Parameters from Fitting SANS Data for 1 wt% $C_{12}E_m$, $m = 5-8$, Solutions in d_5-EAN at Different Temperatures to a Polydisperse Core-Shell Spheres Model[a]

	T (°C)	ϕ	R_c (Å)	t_{shell} (Å)	polydispersity	ρ_{shell} (Å^{-2})	N_{agg}
$C_{12}E_5$	25	0.002	15.4	4.6	0.12	4.1×10^{-6}	44
	47	0.002	16.5	6.4	0.12	4.2×10^{-6}	54
	69	0.002	16.7	6.4	0.12	4.4×10^{-6}	56
$C_{12}E_6$	25	0.002	10.7	2.0	0.12	4.4×10^{-6}	15
	47	0.002	11.2	3.8	0.12	4.7×10^{-6}	17
	69	0.002	12.0	3.6	0.12	4.5×10^{-6}	21
$C_{12}E_8$	25	0.002	10.6	2.4	0.12	4.6×10^{-6}	14
	47	0.003	9.5	2.2	0.12	4.4×10^{-6}	10
	69	0.004	9.0	2.6	0.12	4.5×10^{-6}	9

[a] ϕ, Volume fraction of micelles; R_c, radius of hydrocarbon core; t_{shell}, thickness of ethoxylate shell; ρ_{shell}, scattering length density of the shell; N_{agg}, aggregation number derived from the hydrocarbon core radius and alkyl chain volume. Neither t_{shell} nor ρ_{shell} are reliably determined in these fits; see text.

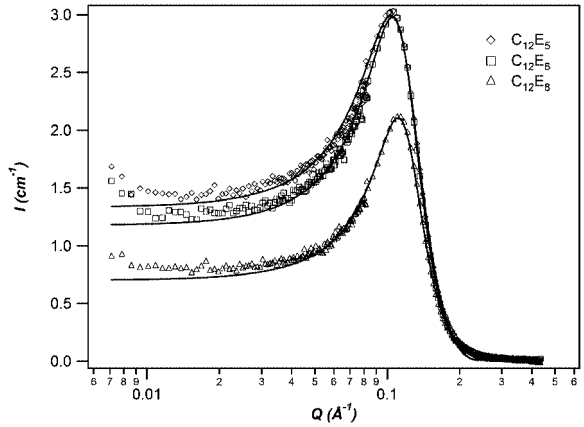

Figure 2. Small angle neutron scattering spectra of 20 wt% solutions of $C_{12}E_5$, $C_{12}E_6$, and $C_{12}E_8$ in $C_2D_5NH_3NO_3$ (d_5-EAN) at 32 °C. Solid lines show fits to a polydisperse core−shell spheres model with excluded volume interactions. Best-fit parameters are listed in Table 2.

Table 2. Derived Parameters from Fitting SANS Data for 20 wt% $C_{12}E_m$, $m = 5-8$, Solutions in d_5-EAN at 32 °C to a Polydisperse Core-Shell Spheres Model with Excluded Volume Interactions

	ϕ	R_c (Å)	t_{shell} (Å)	polydispersity	ρ_{shell} (Å^{-2})	N_{agg}
$C_{12}E_5$	0.22	18.1	6.6	0.14	4.7×10^{-6}	71
$C_{12}E_6$	0.24	17.1	8.0	0.14	4.3×10^{-6}	60
$C_{12}E_8$	0.24	15.9	8.7	0.14	4.5×10^{-6}	48

micelles to comprise a core of (hydrogenous) hydrocarbon-like scattering length density surrounded by a shell of variable scattering length density and radius, dispersed in a pure solvent.[31] The scattering length density of the micelle core, ρ_{core}, was calculated from the scattering lengths and volumes of methyl and methylene fragments of the alkyl chain to be -0.37×10^{-6} Å^{-2}, and ρ_{solv} was calculated from scattering lengths and the density of per-H EAN (1.21 g cm^{-3}) corrected for isotopic substitution to be 4.8×10^{-6} Å^{-2} for $C_2D_5NH_3NO_3$.[30,32,33] The small amounts of dissolved surfactant are not sufficient to affect the coherent scattering length density of the solvent. Structural parameters of $C_{12}E_m$ micelles were obtained by fitting the micelle volume fraction, ϕ, core radius, R_c, shell thickness, t_{shell}, shell scattering length density, ρ_{shell}, and polydispersity. These are listed for $C_{12}E_m$ surfactants in Table 1.

(31) Indeed the scattering is quite well described by a dispersion of homogeneous spheres, yielding radii close to, but slightly larger than, the hydrophobic core radii listed in Table 1. (The fitted volume fraction depends on the assumed scattering length density of these spheres.)

(32) Sears, V. F. *Neutron News* **1992**, *2*, 26.

(33) Allen, M.; Evans, D. F.; Lumry, R. *J. Solution Chem.* **1985**, *14*, 549.

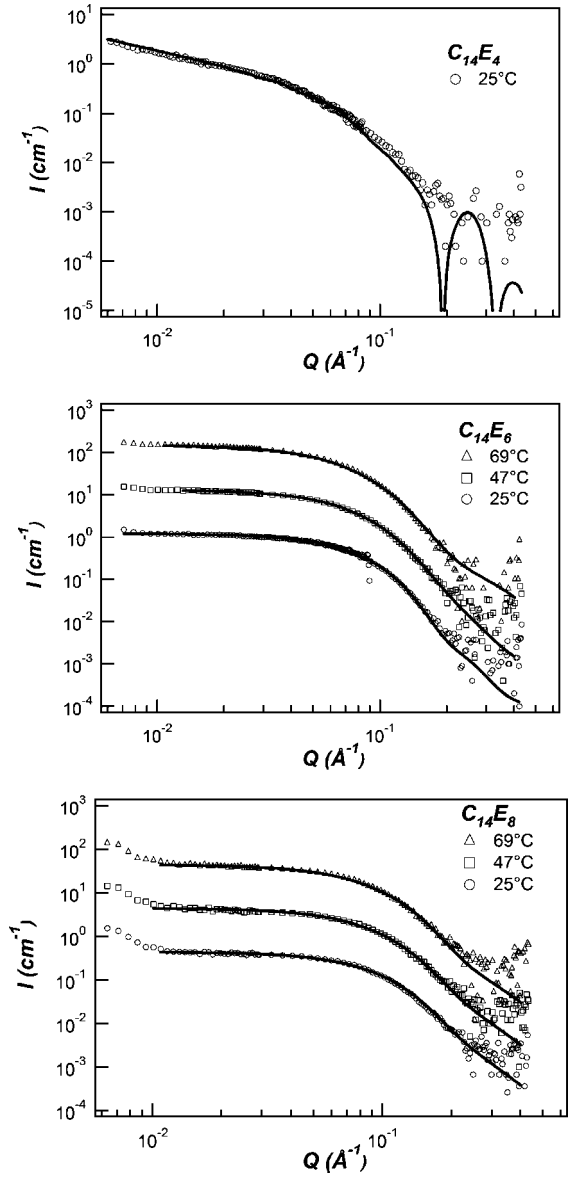

Figure 3. Small angle neutron scattering spectra of 1 wt% solutions of (a) $C_{14}E_4$, (b) $C_{14}E_6$, and (c) $C_{14}E_8$ in $C_2D_5NH_3NO_3$ (d_5-EAN) at 25, 47, and 69 °C. Solid lines show fits to a polydisperse core−shell spheres model for $C_{14}E_6$ and $C_{14}E_8$ and core−shell rods for $C_{14}E_4$, with the parameters listed in Table 3. For clarity, the $C_{14}E_6$ and $C_{14}E_8$ data at 47 and 69 °C were scaled by a factor of 10 and 100, respectively.

Table 3. Best-Fit Parameters to SANS Data for 1 wt% $C_{14}E_m$, $m = 4-8$, Solutions in d_5-EAN at Different Temperatures to a Polydisperse Core-Shell Spheres or Rods Model

	T (°C)	ϕ	R_c (Å)	t_{shell} (Å)	polydispersity	ρ_{shell} (Å^{-2})	N_{agg}
$C_{14}E_4$	25	0.004	20	24	-	4.3×10^{-6}	rods[a]
$C_{14}E_6$	25	0.013	19.1	10.5	0.12	3.4×10^{-6}	72
	47	0.012	18.9	11.4	0.12	3.6×10^{-6}	70
	69	0.012	18.6	11.0	0.12	3.6×10^{-6}	67
$C_{14}E_8$	25	0.009	17.5	9.2	0.12	4.8×10^{-6}	55
	47	0.012	17.0	10.5	0.12	4.8×10^{-6}	51
	69	0.013	17.8	11.3	0.12	4.6×10^{-6}	58

[a] For $C_{14}E_4$ the length of the hydrocarbon core of the rod-like micelles was fitted to be approximately 3×10^4 Å, but this is likely to be a lower bound, as the scattering intensity had not plateaued at the lowest Q. Fits to $C_{14}E_6$ and $C_{14}E_8$ were not very sensitive to t_{shell} or ρ_{shell}; see text.

The coherent scattering is very small for these surfactant solutions ($I < 10^{-1}$ cm^{-1}). This indicates that surfactants are mostly dissolved monomers in solution and that few micelles are present. This is corroborated by the fitted volume fractions of

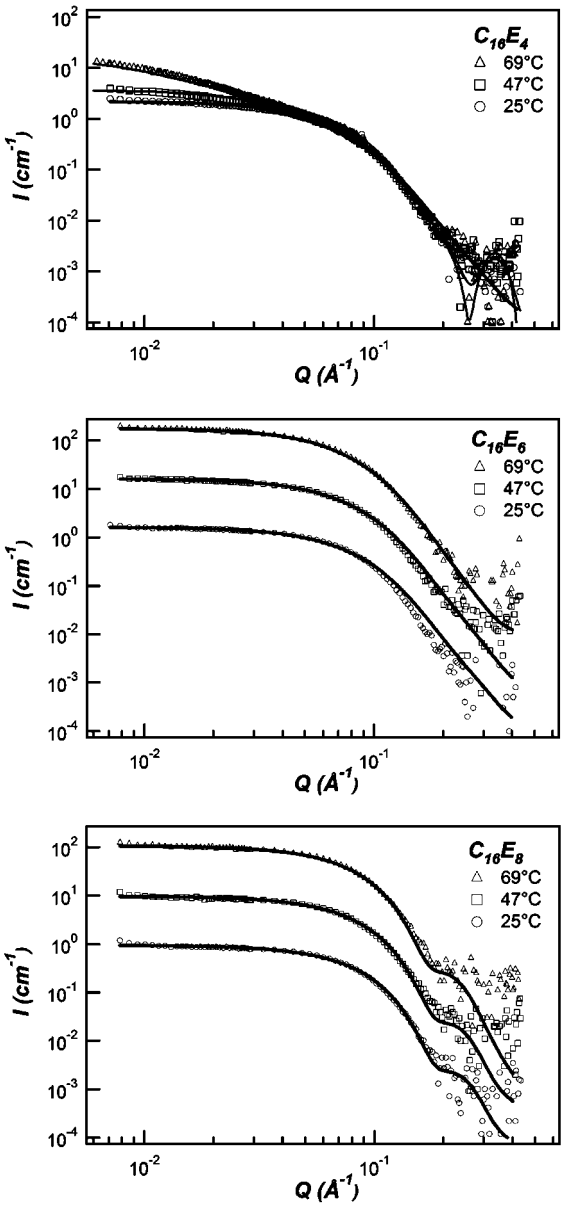

Figure 4. Small angle neutron scattering spectra of 1 wt% solutions of (a) $C_{16}E_4$, (b) $C_{16}E_6$, and (c) $C_{16}E_8$ in $C_2D_5NH_3NO_3$ (d_5-EAN) at 25, 47, and 69 °C. Solid lines show fits to core−shell cylinders or a polydisperse core−shell spheres model with the parameters listed in Table 4 (see text for details). Data and fits for $C_{16}E_6$ and $C_{16}E_8$ have been scaled for clarity.

around 0.002 for all three dodecyl surfactants (Table 1), which is much lower than the total surfactant volume fraction of 0.012.

Table 4. Best-Fit Parameters to SANS Data for 1 wt% $C_{16}E_m$, m = 4, 6, 8, Solutions in d_5-EAN at Different Temperatures to a Polydisperse Core-Shell Spheres or Rods Model

	T (°C)	ϕ	R_c (Å)	t_{shell} (Å)	polydispersity	ρ_{shell} (Å^{-2})	N_{agg}
$C_{16}E_4$	25	0.027	21.3	13.5	0.22	4.4×10^{-6}	88
	47	0.012	15.7	17.3	-	3.4×10^{-6}	~400[a]
	69	0.012	15.7	17.3	-	3.4×10^{-6}	~1600[a]
$C_{16}E_6$	25	0.012	22.6	7.4	0.12	3.2×10^{-6}	105
	47	0.014	22.2	9.4	0.12	3.6×10^{-6}	97
	69	0.015	22.1	10.6	0.12	3.5×10^{-6}	98
$C_{16}E_8$	25	0.008	21.9	7.8	0.12	3.5×10^{-6}	96
	47	0.008	21.3	6.8	0.12	3.8×10^{-6}	88
	69	0.009	21.7	9.3	0.12	$3.3 \times \times 10^{-6}$	93

[a] For $C_{16}E_4$ the length of the hydrocarbon core of the rod-like micelles was fitted to be approximately 120 Å at 47 °C and 500 Å at 69 °C. However no model was entirely satisfactory, and the 47 °C data could also be described by core-shell spheres with a Schulz polydispersity of 0.47.

The critical micelle concentration of these surfactants in EAN is thus inferred to be around a volume fraction of 0.01, or 0.8 wt%.

In fact these scattering spectra are reasonably well described by a range of micelle core radii, shell thicknesses, and polydispersities. The hydrocarbon core radius was in no case greater than the fully extended length of a dodecyl chain of 16.7 Å.[34] As the best-fit mean radius decreases, the corresponding polydispersity increases; hence, we have taken the best fit radius as that which yields the smallest possible polydispersity. In most cases this is comparable with the wavelength spread of the incident neutron beam. These choices will be justified further below, after micellization of longer alkyl chained systems and more concentrated solutions are presented.

SANS spectra of dilute $C_{12}E_5$ solutions in EAN are consistent with a conventional picture of a nonionic micelle, with a core radius between 15.4 Å and 16.7 Å and a corresponding aggregation number, N_{agg}, between 44 and 56. N_{agg} has been calculated by dividing the volume of the homogeneous micelle core, $(4/3)\pi R_c^3$, by the hydrophobic volume of a single chain, v, (350 Å^3 for C_{12}; 405 Å^3 for C_{14}; 460 Å^3 for C_{16}; 515 Å^3 for C_{18}).[34] For $C_{12}E_6$ and $C_{12}E_8$, the core radii and consequently the micelle aggregation numbers are considerably smaller, suggesting much less well-structured aggregates. The fitted shell thicknesses are quite small, and in some cases the scattering length density of the shell is very close to that of d_5-EAN. This may seem to indicate a poorly defined core−shell structure for the micelle but is largely due to the very low scattered intensity above background for dodecyl surfactants.

$C_{12}E_m$ solutions in EAN at higher volume fractions scatter with much greater intensity and clearly show the effects of intermicellar interactions, as shown in Figure 2 for 20 wt% solutions. These spectra were fitted to a polydisperse core−shell model including excluded volume interactions between average micelles, with the best-fit parameters listed in Table 2. As expected for nonionic surfactants in an ionic liquid medium, excluded volume effects are sufficient to describe the intermicellar repulsions. The well-defined scattering peak indicates quite monodisperse micelles, and the fitted polydispersity is comparable with wavelength resolution of the neutron beam. The fitted micelle volume fractions far above the cmc are now consistent with the surfactant concentration, and the micelle core radii of both $C_{12}E_5$ and $C_{12}E_6$ are slightly larger than would be expected for fully extended dodecyl chains. This probably indicates a slight anisotropy in the micelles, as has been reported for aqueous systems. This will introduce a small error in the calculated aggregation numbers for these surfactants. The hydrocarbon core radius of the most polar species, $C_{12}E_8$, remains less than its maximum allowed size.

At this higher surfactant concentration, the shell thickness is more accurately represented, as it determines the excluded volume interaction, whereas in the more dilute, noninteracting solutions it is only detected to the very limited extent that it contrasts with the solvent. The fitted shell thickness here is more consistent with expectations and increases as the ethoxy chain length increases from m = 5 to 8. However, this is still probably an underestimate of the ethoxy layer thickness, as it is derived from the effective distance for hard-sphere contact. As found for the more dilute solutions, the scattering length density of the shell is close to that of the solvent.

The overall radius for the (assumed) spherical micelles, $R_c + t_{shell}$ = 25.1 Å, in EAN is smaller than the 27.6 Å and 33 Å reported previously[21,34] for aqueous $C_{12}E_6$ micelles. Similarly

(34) Tanford, C. *The Hydrophobic Effect*, 2nd ed.; Wiley: New York, 1977.

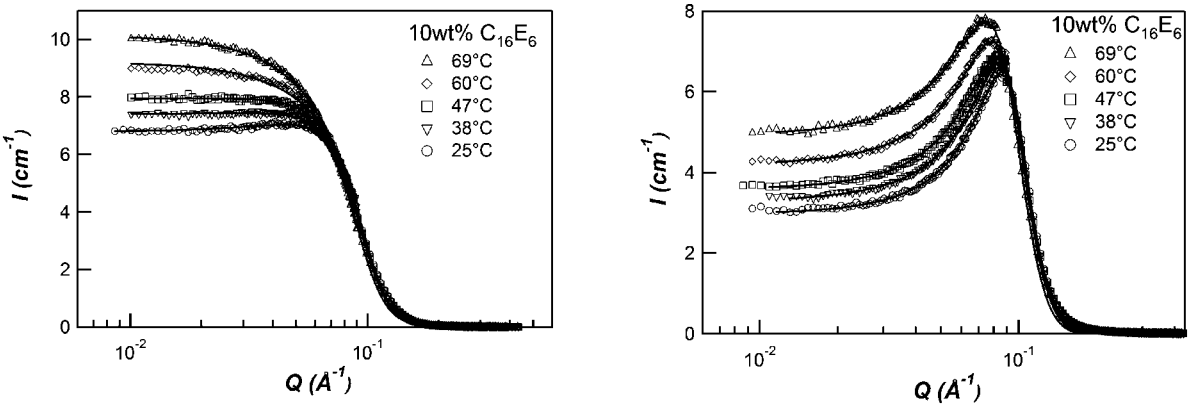

Figure 5. SANS spectra for $C_{16}E_6$ at 10 wt% and 20 wt% in d_5-EAN as a function of temperature. Solid lines show fits of the data to a polydisperse core−shell sphere model with excluded volume interactions (Table 5).

Table 5. Best-Fit Parameters for 10 and 20 wt% $C_{16}E_6$ Solutions in d_5-EAN to a Polydisperse Core-Shell Sphere Model with Excluded Volume Interactions

	T (°C)	ϕ	R_c (Å)	t_{shell} (Å)	polydispersity	ρ_{shell} (Å^{-2})	N_{agg}
10 wt%	25	0.14	24.0	7.6	0.12	3.8×10^{-6}	126
	38	0.13	23.2	7.0	0.19	3.7×10^{-6}	108
	47	0.13	24.0	6.6	0.18	3.7×10^{-6}	126
	60	0.12	22.0	7.5	0.26	3.4×10^{-4}	97
	69	0.13	22.0	8.4	0.25	3.1×10^{-6}	97
20 wt%	25	0.26	21.5	9.0	0.12	3.9×10^{-6}	90
	38	0.26	21.9	8.7	0.12	3.9×10^{-6}	96
	47	0.26	21.2	9.3	0.12	3.5×10^{-6}	87
	60	0.26	20.7	9.6	0.12	3.0×10^{-6}	81
	69	0.27	21.4	10.4	0.12	3.4×10^{-6}	89

for $C_{12}E_8$, we find a 24.6 Å radius in EAN compared with 28 Å and 31 Å reported in water.[19,34] (These studies also reported micelle core radii less than fully extended alkyl chain lengths and hence even more extended ethoxylate chains, but these appear to have been a consequence of assumptions in the fitting procedure.[19])

The "weak" structure and high cmc of $C_{12}E_m$ micelles, compared with their aqueous solution counterparts, are consistent with our previous observation that nonionic surfactants with dodecyl chains do not form lyotropic phases in EAN[15] and only form weakly structured microemulsions when mixed with EAN and alkanes.[16] The solvophobic effect is less strong in EAN than in water; solvophobic alkyl moieties are more soluble, but solvophilic ethoxy groups less well solvated.

$C_{14}E_m$ Surfactants. SANS spectra for 1 wt% solutions of $C_{14}E_4$, $C_{14}E_6$, and $C_{14}E_8$ in d_5-EAN at various temperatures are shown in Figure 3. Scattered intensities are generally greater than for the dodecyl surfactants, indicating a higher concentration of micellized surfactant, although the upturn at low Q observed in $C_{12}E_m$ (Figure 1) remains evident in $C_{14}E_8$. While $C_{14}E_6$ and $C_{14}E_8$ scattering patterns are both consistent with slightly polydisperse core−shell spheres (see Table 3 for fit parameters), $C_{14}E_4$ cannot be fitted to such a model and is best described as core−shell rod-like micelles. This existence of rod-like micelles is strong evidence for the picture of well-structured micelles in EAN formed by solvophobic self-assembly and distinguishes them from simpler unstructured or metastable particles. The progression from spheres to cylinders with decreasing ethoxy number also parallels observations in aqueous systems. Spectra of $C_{14}E_4$ were only recorded at room temperature in this study due to its low cloud point (49 °C in EAN), but temperature-dependent micelle structures are discussed further below.[15]

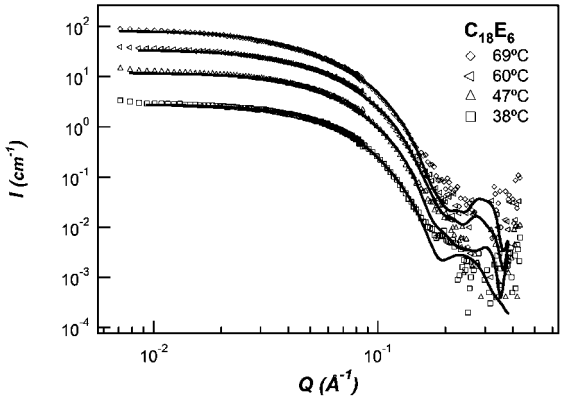

Figure 6. Small angle neutron scattering spectra of 1 wt% solutions of $C_{18}E_6$ in d_5-EAN at 38, 47, 60, and 69 °C. Solid lines show fits to a core−shell rod-like micelles model with the parameters listed in Table 6. Higher temperature data were scaled for clarity.

For $C_{14}E_6$, the fitted hydrocarbon core radius is close to the expected value of 19.3 Å for a fully extended tetradecyl chain. Like $C_{12}E_8$, the core radii of $C_{14}E_8$ are smaller than the fully extended alkyl chain at all temperatures examined. In contrast with the ambiguities in interpreting scattering by dilute solutions of $C_{12}E_m$ surfactants, $C_{14}E_m$ clearly form structures recognizably similar to conventional aqueous micelles but with slightly smaller aggregation numbers. The progression toward higher aggregate curvature with increase in headgroup size from $C_{14}E_4$ to $C_{14}E_8$, first from rods to spheres and then decreasing core radius and aggregation number is just what would be expected for micelles formed with a well-defined and segregated hydrocarbon core.

In these systems the fitted volume fraction, which includes the surfactant and any solvent incorporated among the ethoxylate chains, is greater than the volume fraction of "dry" surfactant in the solution. This indicates that most of the surfactant is present in the form of micelles, and that the cmc is much less that 1 wt%. The fitted shell thicknesses and scattering length densities are consistent with strong incorporation of EAN into the ethoxy head groups, so that there is little neutron contrast between the shell and solvent. This affects the fitted volume fraction, and the fits are not particularly sensitive to shell thickness. Higher concentrations of the tetradecyl surfactants were not examined here. Lyotropic phases of tetradecyl surfactants are marginally stable;[15] $C_{14}E_4$ forms a lamellar phase and $C_{14}E_8$ forms a hexagonal phase at room temperature, whereas $C_{14}E_6$ forms neither. Both phases melt at only modest temperatures.

$C_{16}E_m$ Surfactants. Figure 4 shows the SANS spectra for 1 wt% solutions of $C_{16}E_4$, $C_{16}E_6$, and $C_{16}E_8$ in d_5-EAN. The scattered intensities are comparable with those of the $C_{14}E_m$ series, as are the fitted volume fractions, and the results for this series reinforce

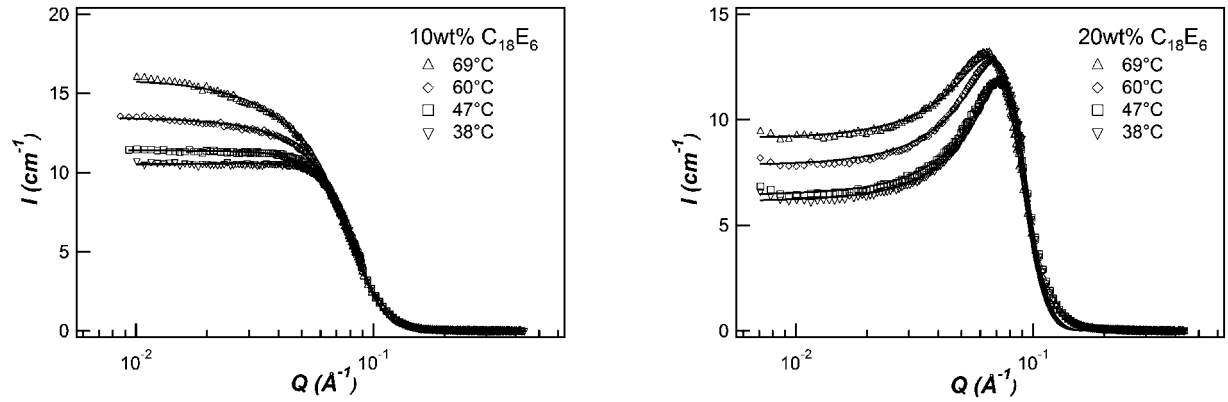

Figure 7. Small angle neutron scattering spectra of 10 and 20 wt% solutions of $C_{18}E_6$ in d_5-EAN at 38, 47, 60, and 69 °C. Solid lines show best-fits to a polydisperse core−shell spheres with hard-sphere interactions.

Table 6. Derived Parameters from Fitting SANS Data for 1 wt% $C_{18}E_6$ Solutions in d_5-EAN at Different Temperatures to a Core-Shell Rod-Like Micelle Model

surfactant	T (°C)	ϕ	R_c (Å)	t_{shell} (Å)	L_c[a] (Å)	ρ_{shell} (Å^{-2})	N_{agg}
$C_{18}E_6$	38	0.014	20.7	7.3	69	3.4×10^{-6}	159
	47	0.013	20.8	7.4	77	3.6×10^{-6}	184
	60	0.013	20.1	7.2	92	3.3×10^{-6}	214
	69	0.015	18.4	9.4	110	3.0×10^{-6}	211

[a] L_c is the core length.

the trends observed in the tetradecyl surfactants. $C_{16}E_4$ shows clear evidence of a change in micelle morphology on warming toward its cloud point (88 °C[15]). While its scattering is well-described by polydisperse core−shell spheres at 25 °C, the micelles become anisotropic and gradually grow into elongated rods on warming. A characteristic Q^{-1} decay in the scattered intensity is evident at 69 °C. In contrast, the scattering from $C_{16}E_6$ and $C_{16}E_8$ change very little over the temperature range examined, and are well-described by core−shell spheres, as would be expected from nonionic surfactants with larger head groups and far below their cloud points. The best-fit radii of the hydrocarbon cores are close to the expected extended alkyl chain length of 21.7Å for $C_{16}E_6$ and $C_{16}E_8$.

SANS spectra for $C_{16}E_6$ at both 10 and 20 wt% are shown in Figure 5, together with fits to a polydisperse core−shell model with excluded volume interactions. At 10 wt% a small interaction peak is apparent at 25 °C, but this disappears on warming. At 20 wt% an interaction peak is clearly observed at all temperatures. As temperature is increased, this moves to lower Q, consistent with fewer, larger micelles.

Table 5 summarizes the best-fit parameters for the concentrated $C_{16}E_6$ solutions. At these concentrations micelle core radii are slightly larger, but this may actually be due to the micelles becoming slightly anisotropic. The length of the ethoxy chains are similar to those obtained in 1 wt% solutions and also to the fitted thicknesses of $C_{14}E_6$ and concentrated $C_{12}E_6$ micelles. Reasonable fits could be obtained with core radii up to 1.5 Å longer than the fully extended chain, with a corresponding decrease in t_{shell} such that the overall micelle radius remains virtually unchanged. There is little change in micelle core radius or aggregation number with increasing concentration up to 20 wt%. The fits also suggest that the average micelle size does not change significantly with temperature, but that the shift in peak position and low Q scattering is a consequence of increased micelle polydispersity. Of course, this necessarily includes the formation of larger micelles, and it is not possible to discern whether slightly anisotropic micelles are being formed. Although the fits shown in Figure 5 are not really satisfactory, they are sufficient to show trends; we have not attempted to model these concentrated spectra with interacting spheroidal micelles.

$C_{18}E_6$. SANS spectra of $C_{18}E_6$ micellar solutions at various concentrations and temperatures in d_5-EAN are shown in Figure 6. ($C_{18}E_6$ is not soluble in EAN at room temperature.) Dilute solution scattering spectra were best fit by (short) core−shell rods, also shown. Fit parameters, listed in Table 6, show that the micelles become slightly more anisotropic as temperature is increased, increasing the scattered intensity at low Q.

As noted in concentrated $C_{12}E_m$ and $C_{16}E_6$ solutions, 10 and 20 wt% solutions of $C_{18}E_6$ show scattering peaks due to intermicelle interference effects. At 10 wt% the small peak disappears as the temperature is raised, but at 20 wt% the peak shifts to lower Q on warming.[36]The fitted parameters show negligible effect of temperature on micelle size, which is consistent with a 24.3 Å core radius (corresponding to an aggregation number of 117). As observed in $C_{16}E_6$, the change in scattering spectrum on warming is best described by an increase in the polydispersity, a decrease in the scattering length density of the shell (from 2.5 to 2.0×10^{-6} Å^{-2}) and a slight decrease in volume fraction of micelles (0.13−0.11 and 0.23−0.19, respectively), which we interpret as exclusion of d_5-EAN from the ethoxylate headgroup shell.

Discussion

These experiments have shown that C_nE_m surfactants in EAN aggregate into conventionally structured micelles with a solvophobic, hydrocarbon core surrounded by a corona of ethoxy groups. Several trends emerge from the observed micelle structure in EAN as a function of alkyl chain length, ethoxy chain length, and temperature.

Micelles formed by dodecyl-chained surfactants are weakly structured, at least in dilute solution, such that a core−shell micelle structure cannot be unambiguously discerned. However, the presence of aggregates leading to solution structure at higher concentrations is clear. Increasing the alkyl chain length to fourteen or longer leads to the formation of much better-defined aggregates, very similar to aqueous micelles. This is broadly consistent with our observations of the patterns of lyotropic phase formation by nonionic surfactants in EAN, in which an offset of about four methylenes is required to reconcile differences between water and EAN.

The effect of increasing ethoxy chain length is also consistent with truly structured micelles in EAN. Using the packing

(35) Zulauf, M.; Weckstrom, K.; Hayter, J. B.; Degiorgio, V. *J. Phys. Chem.* **1985**, *89*, 3411.
(36) Aswal, V. K.; Goyal, P. S. *Phys. Rev. E* **2000**, *61*, 2947.

parameter concept to understand micelle morphology, v/a_0l_c,[18] as the size of the ethoxy group increases, so does a_0, and the micelle shape is expected to change from planar (bilayers or disks) to rods and on to spheres. Just such a shape transition from rods to spheres is clearly seen in tetradecyl and hexadecyl surfactants as the number of ethoxy units increases from four to six.

A change in micelle morphology from spheres to rods upon warming $C_{16}E_4$ also closely parallels observations in aqueous systems on e.g. $C_{12}E_5$ and $C_{12}E_6$.[37] As noted previously, the existence of a lower consolute boundary for nonionic surfactants in EAN was unexpected and will be the subject of further investigation.

Nonionic surfactants tend to form more highly curved aggregates in EAN than in water; $C_{16}E_6$ forms long, cylindrical micelle in aqueous solution but globular aggregates in EAN. This might simply be attributed to the proximity of its aqueous cloud point of 36 °C (in D_2O[38]), compared with 130 °C in EAN, but the trend is actually much more widespread. $C_{16}E_4$ grows into cylinders on warming in EAN but forms only a lamellar phase in aqueous solution, and L_3 at elevated temperatures.[22] $C_{12}E_5$ and $C_{12}E_6$ form globular micelles in EAN but cylinders in water.

A larger headgroup area seems to run contrary to the thinner and more compact ethoxylate shell observed in EAN compared with aqueous micelles. This might easily arise from two considerations. First, compressing the oligomeric ethoxy chain may simply lead to greater steric repulsion between neighboring head groups. However this effect may also be enhanced by solvation of the ethoxy groups by the large ethylammonium cations and possibly by their associated nitrate counterions. The molecular volume of an EAN ion-pair (150 Å^3) is much greater than H_2O (30 Å^3), so even much lower solvation numbers can lead to greater solvation volume. We have recently reported a similar effect in nonionic microemulsions with EAN as the polar phase.[16]

Acknowledgment. This work was supported by the Australian Research Council. This work utilized facilities supported in part by the National Science Foundation under Agreement No. DMR-0454672. We acknowledge the support of the National Institute of Standards and Technology, U.S. Department of Commerce, in providing the neutron research facilities used in this work.

LA801603T

(37) Glatter, O.; Fritz, G.; Lindner, H.; Brunner-Popela, J.; Mittelbach, R.; Strey, R.; Egelhaaf, S. U. *Langmuir* **2000**, 16.

(38) Schurtenberger, P.; Cavaco, C.; Tiberg, F.; Regev, O. *Langmuir* **1996**, *12*, 2894.